Deformation corrected real-time terahertz imaging

Deformation corrected real-time terahertz imaging

Toshiaki Hattori[a) and Masaya Sakamoto

Institute of Applied Physics, University of Tsukuba, 1-1-1 Tennodai, Tsukuba, Ibaraki 305-8573, Japan

The authors have developed a method of real-time terahertz imaging in which image deformation due to nonuniformity of residual birefringence in the electro-optic (EO) sampling crystal is corrected. Real-time terahertz imaging using intense terahertz pulses and two-dimensional EO sampling can suffer from birefringence nonuniformity of the EO crystal since the birefringence is explicitly used for the linear detection of the terahertz field. In the proposed method, the distribution of the residual birefringence of the EO crystal is measured and used for image correction. Deformation-free images of the spatial profile of a focused terahertz pulse were obtained. © 2007 *American Institute of Physics.* [DOI: 10.1063/1.2752543]

Imaging using terahertz radiation has been attracting considerable interest since the demonstration by Hu and Nuss.[1] Use of intense terahertz pulses and a two-dimensional electro-optic (EO) sampling method enables real-time acquisition of the terahertz images.[2–20] Typical setup uses amplified femtosecond mode-locked Ti:sapphire laser pulses to pump a large-aperture photoconductive antenna for generation of the intense terahertz pulses. Detection of spatial distribution of terahertz electric field is made using a large EO crystal, an expanded probe beam, and an optical image detector. Two configurations of the optical setup have been used for the detection of the polarization change of the probe light due to the EO effect induced by the terahertz field. One configuration is composed of crossed polarizer and analyzer,[2–13,18,19] and an EO crystal between them. Detection of signal that is linear to the terahertz field is enabled using residual birefringence of the EO crystal.[21] The other configuration uses a quarter-wave plate (QWP) and an analyzer that is oriented at a small angle from the crossed position.[15–17,20] The balanced detection method,[22] which is widely used for wave form measurements, is not used in image detection. In both configurations, nonuniformity of residual birefringence of the EO crystal affects the image quality. In this letter, we present a method of real-time detection of two-dimensional distribution of the terahertz field, in which birefringence nonuniformity of the EO crystal is directly measured and the obtained terahertz image is corrected for it.

In the configuration of EO sampled imaging using crossed polarizers, the intensity of the probe light transmitted through the analyzer can be expressed as[21]

$$I = I_0[(\theta + \Gamma)^2 + \eta], \tag{1}$$

where I_0 is the incident light intensity, θ is the phase retardation due to the EO effect, which is proportional to the terahertz field, Γ is the phase retardation due to residual birefringence of the EO crystal, and η is the depolarization factor due to scattering and other types of imperfection in the optics. It is assumed here that $|\theta|$ and $|\Gamma| \ll 1$. In this method, nonuniformity of Γ directly affects the uniformity of the obtained image, and the magnitude of Γ cannot be controlled although there is an appropriate value of Γ for the largest signal modulation depth.[21] In the configuration using a QWP

and a tilted analyzer,[15,16,23–25] on the other hand, the transmitted light intensity becomes

$$I = I_0[(\theta + \delta)^2 + \eta], \tag{2}$$

which is the same as above except that Γ is replaced by the tilt angle of analyzer δ. Derivation of Eq. (2) is detailed in the appendix of Ref. 16, where residual birefringence of the EO crystal is not taken into account. By taking into account the phase retardation due to residual birefringence of the EO crystal, we obtain

$$I = I_0[(\theta + \delta + \Gamma)^2 + \eta]. \tag{3}$$

In Eqs. (2) and (3), it is assumed that $|\theta|$, $|\delta|$, and $|\Gamma| \ll 1$. In the linear region, i.e., when $|\theta| \ll |\delta + \Gamma|$, the phase retardation due to the terahertz field is obtained as

$$\theta = (I - I_b)/[2(\delta + \Gamma)I_0], \tag{4}$$

where I_b is background light intensity obtained without the terahertz field. It is seen from this expression that the sensitivity of the measurement is a function of the residual birefringence at each point. For spectroscopic object imaging,[12,13] the signal intensity can be divided by a reference intensity, which leads to images immune to the nonuniformity. For the measurements, however, of terahertz field profiles, the influence cannot be removed.

In a method presented here, we measured the distribution of the residual birefringence by acquiring the background intensity I_b at several rotation angles δ of the analyzer. By fitting the data to a quadratic function of δ according to Eq. (3), I_0, Γ, and η were obtained at each pixel of the image.

Experiments were performed using a setup similar to that reported previously.[15] Regeneratively amplified Ti:sapphire laser pulses at 800 nm irradiated the 3 cm gap between the electrodes of a large-aperture semi-insulating GaAs photoconductive antenna at a repetition rate of 1 kHz. The probe beam was split from the pump beam and passed through a polarizer before combined with the terahertz beam by a pellicle beam splitter. Then it passed through a 1 mm thick, 20×20 mm^2 $\langle 110 \rangle$ ZnTe crystal, a QWP, an analyzer, and an imaging optics before detected by a charge coupled device camera.

Before describing the effect of nonuniformity correction, we present first a result of frequency-resolved object imaging in Fig. 1. The object was 2 mm lines and spaces of alumi-
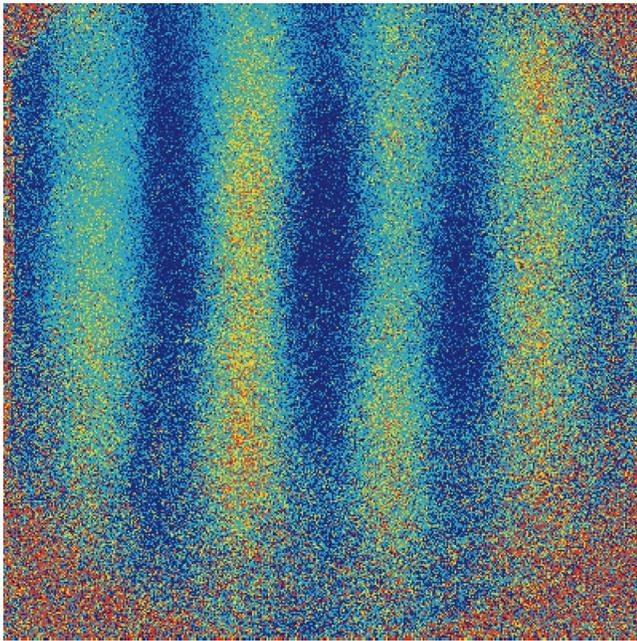
a)Electronic mail: hattori@bk.tsukuba.ac.jp

FIG. 1. (Color online) Frequency-resolved terahertz image of 2 mm lines and spaces of aluminum at 0.5 THz. Distribution of Fourier amplitude divided by that of a reference image is shown. The image area corresponds to the crystal size of 20×20 mm^2.

num foils on paper. The spatial profile of the object was imaged by a TPX lens of a focal length of $f = 98.3$ mm to the ZnTe crystal. Distances between the object and the lens and between the lens and the ZnTe crystal were $9f/4$ and $9f/5$, which leads to 5:4 imaging. The probe delay was scanned and the obtained temporal terahertz wave form at each pixel was Fourier transformed to obtain frequency-resolved images, which were then divided by a reference image that was obtained using a blank sample. Figure 1 shows the distribution of the Fourier amplitude of the terahertz field at 0.5 THz. Because of the division by the reference, any image deformation due to EO crystal birefringence is automatically corrected. Thus it is seen that EO crystal nonuniformity is not a serious problem in object imaging, and that resolution better than 1 mm is obtained using this imaging setup.

    We obtained the distribution of the phase retardation due to the residual birefringence of the ZnTe crystal used in the measurements and that of the scattering term following the procedure described above. Results are shown in Fig. 2. It was found that Γ ranged from -0.05 to 0.05 in this crystal
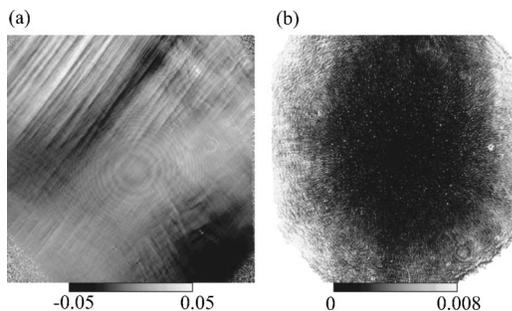

FIG. 2. (a) Distribution of the phase retardation of the probe light Γ due to residual birefringence of the EO crystal. (b) Distribution of the scattering term η. In both images, the area corresponds to the crystal size of 20×20 mm^2. Data quality of the four corners are poor because of low probe intensity.
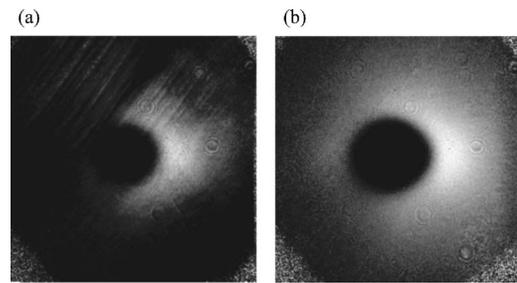

FIG. 3. Distribution of the electric field of a focused terahertz pulse at a positive delay time. (a) Image obtained without taking into account the influence of residual birefringence of the ZnTe crystal. (b) Image corrected for the residual birefringence.

and stripe structures were clearly seen. Scattering factor η was distributed around 0.001 in the major central part fo the image area, and reached $\eta \simeq 0.005$ at some bright spots. In the following terahertz image measurements, δ was set at 3° (0.052 rad) to avoid the condition that $\delta + \Gamma = 0$ and ensure linear detection of the terahertz field.

    For the field profile imaging, the terahertz pulses were focused by the TPX lens, and the ZnTe crystal was placed at the focal point. The probe delay was set at a time after the peak to observe a ring profile.[14] In Fig. 3(a) is shown the terahertz field distribution obtained by assuming no residual birefringence. It is seen that the image is seriously affected by the nonuniformity of the residual birefringence. Figure 3(b) shows an image corrected for the residual birefringence, which is almost free from the effect of birefringence nonuniformity.

    In another approach, Γ was estimated from the background light intensity. As proposed by Jiang and Zhang,[8] when η can be neglected, we can obtain the background retardation as

$$\delta + \Gamma = \sqrt{I_b/I_0}, \tag{5}$$

and the terahertz field signal is obtained by

$$\theta = (I - I_b)/(2\sqrt{I_0 I_b}). \tag{6}$$

In this method, separate measurements of Γ is not necessary although we need to perform measurements at a larger δ in order to ensure the condition $(\delta + \Gamma)^2 \gg \eta$ at every pixel of the image. Images obtained at $\delta = 1°$, 2°, and 4° are shown in Figs. 4(a)–4(c), respectively. The results show that a tilt angle of 1° or 2° is not sufficiently large to get rid of the effect of birefringence nonuniformity since $\delta + \Gamma$ can vanish at some positions. At $\delta = 4°$, better correction was obtained although it is not so good as that for the image shown in Fig. 3(b). Furthermore, noise becomes larger and saturation takes place because the transmitted probe intensity is larger at $\delta = 3°$. Thus it can be concluded that image quality obtained using the method based on estimation of Γ from the background intensity is not so good as that based on direct measurement of Γ although this method is simple and easy.

    In conclusion, we proposed and demonstrated a method for real-time terahertz imaging in which image deformation due to nonuniformity of the residual birefringence of the EO crystal is corrected. Distribution of residual birefringence and scattering factor were directly measured and used for the image correction. Clean images of the terahertz pulse profiles almost free from deformation were obtained using this method.
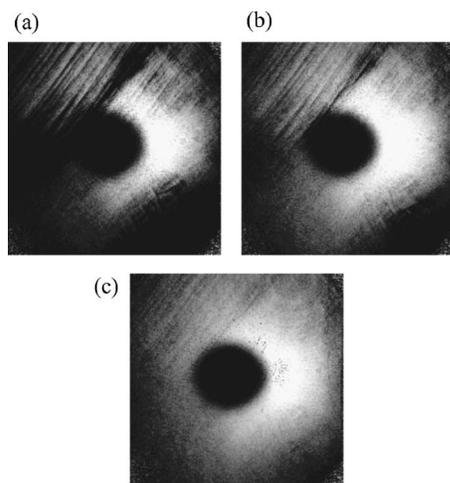
FIG. 4. Terahertz field profile images obtained by estimating Γ from the background light intensity. The analyzer tilt angles δ were (a) 1°, (b) 2°, and (c) 4°.

[1] B. B. Hu and M. C. Nuss, Opt. Lett. **20**, 1716 (1995).
[2] Q. Wu, T. D. Hewitt, and X.-C. Zhang, Appl. Phys. Lett. **69**, 1026 (1996).
[3] Z. G. Lu, P. Campbell, and X.-C. Zhang, Appl. Phys. Lett. **71**, 593 (1997).
[4] Z. Jiang and X.-C. Zhang, Appl. Phys. Lett. **72**, 1945 (1998).
[5] Z. Jiang and X.-C. Zhang, Opt. Lett. **23**, 1114 (1998).
[6] Z. Jiang, F. G. Sun, and X.-C. Zhang, Opt. Lett. **24**, 1245 (1999).
[7] Z. Jiang and X.-C. Zhang, Opt. Express **5**, 243 (1999).
[8] Z. Jiang and X.-C. Zhang, IEEE Trans. Microwave Theory Tech. **47**, 2644 (1999).
[9] Z. Jiang, X. G. Xu, and X.-C. Zhang, Appl. Opt. **39**, 2982 (2000).
[10] M. Usami, T. Iwamoto, R. Fukasawa, M. Tani, M. Watanabe, and K. Sakai, Phys. Med. Biol. **47**, 3749 (2002).
[11] M. Usami, R. Fukasawa, M. Tani, M. Watanabe, and K. Sakai, Electron. Lett. **39**, 1746 (2003).
[12] M. Yamashita, M. Usami, K. Fukushima, R. Fukasawa, C. Otani, and K. Kawase, Appl. Opt. **44**, 5198 (2005).
[13] M. Usami, M. Yamashita, K. Fukushima, C. Otani, and K. Kawase, Appl. Phys. Lett. **86**, 141109 (2005).
[14] R. Rungsawang, K. Ohta, K. Tukamoto, and T. Hattori, J. Phys. D **36**, 229 (2003).
[15] T. Hattori, K. Ohta, R. Rungsawang, and K. Tukamoto, J. Phys. D **37**, 770 (2004).
[16] R. Rungsawang, K. Tukamoto, and T. Hattori, Jpn. J. Appl. Phys., Part 1 **44**, 1771 (2005).
[17] R. Rungsawang, A. Mochiduki, S. Ookuma, and T. Hattori, Jpn. J. Appl. Phys., Part 2 **44**, L288 (2005).
[18] F. Miyamaru, T. Yonera, M. Tani, and M. Hangyo, Jpn. J. Appl. Phys., Part 2 **43**, L489 (2004).
[19] T. Yasuda, T. Yasui, T. Araki, and E. Abraham, Opt. Commun. **267**, 128 (2006).
[20] J. van Tilborg, C. B. Schroeder, Cs. Tóth, C. G. R. Geddes, E. Esarey, and W. P. Leemans, Opt. Lett. **32**, 313 (2007).
[21] Z. Jiang, F. G. Sun, Q. Chen, and X.-C. Zhang, Appl. Phys. Lett. **74**, 1191 (1999).
[22] A. Nahata, A. S. Weling, and T. F. Heinz, Appl. Phys. Lett. **69**, 2321 (1996).
[23] G. L. Eesley, M. D. Levenson, and W. M. Tolles, IEEE J. Quantum Electron. **14**, 45 (1978).
[24] M. D. Levenson and G. L. Eesley, Appl. Phys. **19**, 1 (1979).
[25] D. McMorrow, W. T. Lotshaw, and G. A. Kenney-Wallace, IEEE J. Quantum Electron. **24**, 443 (1988).